J. Geophys. 49, 57–65 (1981)

Journal of Geophysics

A Crustal Gravity Model of the Mare Serenitatis – Mare Crisium Area of the Moon

P. Janle

Institut für Geophysik der Universität, Bundesstr. 55, D-2000 Hamburg 13, Federal Republic of Germany and
Institut für Geophysik der Universität, D-2300 Kiel, Federal Republic of Germany

Abstract. Several published mass configurations of mascon models have been used to calculate and compare gravity models for Mare Crisium. The calculations are based on line-of-sight (LOS) gravity data from the Apollo missions. A new model consisting of mare basalts, a crust-mantle mix, and a mantle plug is presented. Additionally, an isostatic model has been developed. A detailed regional model from southern Imbrium over Mare Serenitatis to Mare Crisium has been calculated, based upon the new model. Crustal thickenings have been introduced in order to fit the gravity lows bordering the mare basins.

A discussion of the stability of the mascons, presented in this paper, leads to the following conclusions: (1) the average postmare upper mantle viscosity must be greater or equal to 10^{27} poise; (2) high temperature models seem to be inappropriate considering this high viscosity and the mascon shear stresses of 65 bar at a depth of 200 km. The second statement could be revised in the light of investigations of a totally dry rheology.

Key words: Crustal gravity models – Lunar mascons – Lunar upper mantle rheology.

Introduction

Since lunar line-of-sight (LOS) gravity data derived from spacecraft Doppler tracking signals have been available, several methods of gravity modelling have been developed. Conventional geophysical computation of the vertical gravity component of a given mass model is not possible (1) because of the line-of-sight nature of the data and (2) because of the least squares procedure of orbit determination which introduces an amplitude compression of 25%–30%. The methods and problems of data acquisition and reduction are described by Gottlieb (1970) and Sjogren et al. (1976).

There are three methods for computing LOS gravity of given mass configurations: (1) direct dynamic modelling of a gravity anomaly with a complex orbit determination program (Michael and Blackshear 1972), (2) dynamic estimation of the acceleration vectors and a subsequent static gravity modelling of the vectors (Bowin et al. 1975), and (3) a quasi-dynamic modelling with a simplified orbit simulation program. Method 3 and a comparison of all three methods are described by Phillips et al. (1978). Methods 1 and 2 require large computational times, while method 3, the one used in this paper, is comparatively fast.

The first Doppler gravity profiles of the moon received revealed large positive gravity anomalies associated with most circular maria (Muller and Sjogren 1968). These gravity maxima were explained by mass concentrations (mascons) soon after their discovery. Several models have been developed to describe the mascon anomalies. Most are based on mass excesses, but there are also some mass configurations which are in isostatic equilibrium.

The purpose of this paper is

(1) to compare old models of mass surpluses with each other and to develop a new model,

(2) to present an isostatic model,

(3) to develop a complete crustal model extending from the Apennines area over Mare Serenitatis to Mare Crisium, based on LOS gravity data from orbits of different heights.

Gravity Data and Boundary Conditions

The observational data for model fitting are low and high altitude LOS gravity data from the Apollo 15 Command and Service Modules (CSM), revolutions 5 and 15. The spacecraft altitudes are about 12–20 km for revolution 5 and 100–110 km for revolution 15. Gravity data for two different altitude levels permit a refined model fitting of possible model configurations. The profile location is shown in Fig. 1.

In addition to the LOS gravity data, there are several boundary conditions which influence the model parameterization

- topography of the mare basins,
- mean crustal thickness,
- density-depth distribution,
- thickness of mare basalts,
- initial depth of the impact basins.

These conditions will now be discussed in detail.

The gravity effects of the mare basin topography have a large influence on quantitative mass modelling. The basins of Serenitatis and Crisium contribute −89 mgal and −140 mgal to the measured gravity for revolution 5 in the central areas. This increases the gravity anomaly which has to be fitted by 40%–70% (Fig. 2). Several older published models ignore these topographic effects.

The mean altitude levels of the surroundings of the Serenitatis and Crisium areas and of the basins themselves have been determined from modern Lunar Topographic Orthophotomaps (LTO, Schimerman 1973). The values of the altitude levels are given as distance from the center of mass of the moon:

surroundings:	1,736.0 km,
Crisium basin:	1,733.7 km,
Serenitatis basin:	1,734.35 km.

0340-062X/81/0049/0057/$01.80

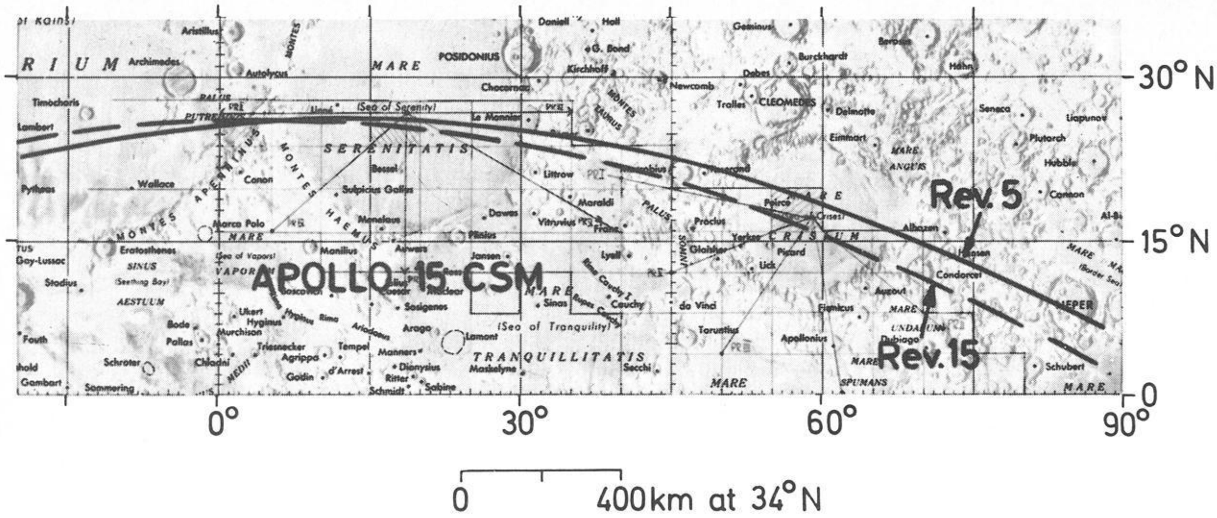

Fig. 1. Profile location, Apollo 15 Command and Service Modules (CSM), *Rev. 5 and 15*. Spacecraft altitudes: *Rev. 5:* 12–20 km; *Rev. 15:* 100–110 km

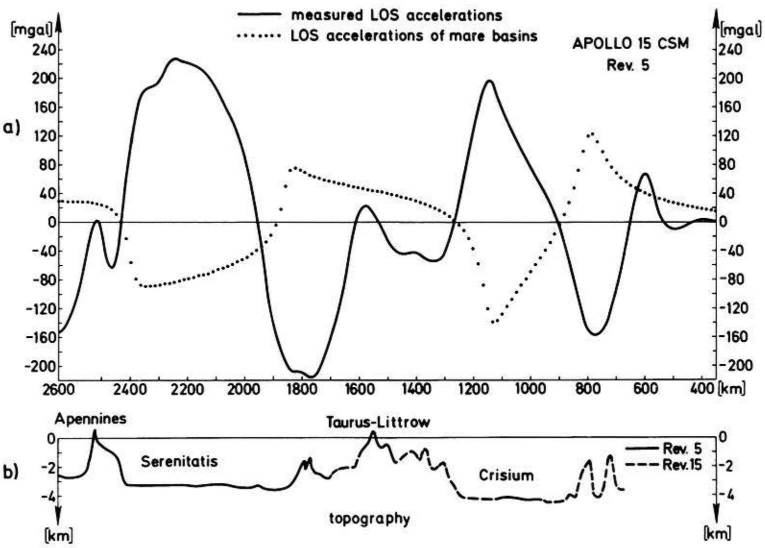

Fig. 2a and b. Line of sight (*LOS*) gravity effect of mare basin topography, *Appollo 15 CSM, Rev. 5.*
a Measured LOS accelerations and calculated LOS accelerations of mare basin topography
b topography from Lunar Topographic Orthophotomaps (LTO); zero level of elevation scale is related to a mean lunar radius of 1,738 km

The zero level of all elevation and depth scales in the figures is related to a mean lunar radius of 1,738 km.

A mean crustal thickness of 60 km has been assumed for the nearside of the moon. This value has been derived from seismic investigations (Toksöz et al. 1974).

The mean density-depth distribution of the crust and upper mantle is based upon petrologic models, seismic models, and rocks returned to Earth (Cooper et al. 1974; Solomon 1974). Following these investigations a density of 2.7 g/cm^3 has been assumed for the upper crust with density increasing to 3.0 g/cm^3 for the lower crust. A value of 3.3 g/cm^3 has been adopted for the mare basalts. A decrease of the mean density to 2.4 g/cm^3 has been assumed for the uppermost layers to a depth of 3–4 km presumed due to the loosening by impacts in agreement with measurements of Talwani et al. (1973) on returned samples. According to Solomon (1974), the upper mantle density should be rather high and is assumed here to be 3.5 g/cm^3. A boundary condition for the thickness of the mare basalts has been adopted from investigations by De Hon and Waskom (1976). They found a maximum thickness of 1–2 km in the shelf areas of the mare basins from rim height estimations for impact craters partially buried by mare basalts. A further confirmation of this result is given by Andre et al. (1979) from orbital X-ray data. According to Hörz (1978) the mare basalt thicknesses found by De Hon and Waskom (1976) should be reduced by a factor of 2. Thus the maximum thickness of the mare basalts should be much less than 10 km. A maximum value of 7 km is used in this paper.

Each mascon model proposed must be in accordance with a reasonable model history, which depends on the initial depth of the impact basin. Estimations of this depth differ over a very large range: Head et al. (1975) estimate for Imbrium a value of 8–27 km, while Dence (1977) assumes, for the same basin, 160 km. Thus this boundary condition cannot provide much constraint in model construction.

Values of the boundary conditions are summarized in Table 1.

Non-Isostatic Mascon Models

In this section some basic non-isostatic mascon model solutions from the literature are presented and a further development of these models is described for the mascons of Mare Crisium and

Table 1

Topography (mare basin depth)	2.3 km	Crisium
	1.65 km	Serenitatis
Mean crustal thickness	60 km	
Density-depth distribution	2.4 g/cm^3	uppermost crust
	2.7 g/cm^3	upper crust
	2.9–3.0 g/cm^3	lower crust
	3.3 g/cm^3	mare basalts
	3.5 g/cm^3	upper mantle
Thickness of mare basalts	$\leqq$ 1–2 km	shelf areas
	$\leqq$ 7 km	central areas
Initial depth d of the impact basins	10 km $< d <$ 160 km	

Mare Serenitatis. A similar investigation has been presented by Sjogren and Smith (1976) for the Orientale basin.

All models have been fitted to the gravity maxima of both Crisium and Serenitatis in order to take into account the long distance effects of gravity. As a first step, the mass models have been fitted to the high altitude orbit Apollo 15 CSM, revolution 15. Different model solutions for Crisium are given in Fig. 3.

Nearly all models (except the "mixed crust model" of Fig. 3d) originate from a medium depth of the initial impact basin of several tens of kilometers.

Figure 3a represents the near surface solution (Conel and Holstrom 1968). The mare basalt thickness of 26.5 km is considerable and not compatible with the boundary condition of thin mare basalts.

The mantle plug solution of Wise and Yates (1970) is presented in Fig. 3b. It is assumed in this model that the mare basalts have no excess density or are negligibly thin. Relative large vertical movements of the crust-mantle boundary are necessary in order to explain a mantle plug of 40 km. Two processes could be responsible for a Moho rise: (1) rebound immediately after the impact and (2) later isostatic adjustment.

Figure 3c shows the two-body mare basalts and mantle plug model previously suggested by Bowin et al. (1975). In order to observe the boundary condition of 7 km mare basalt thickness, a mantle plug of 25 km is required.

In Fig. 3d a mixed crust consisting of crustal and intruded mantle material is introduced in addition to a thin mare basalt layer. Intrusions of mantle material into the crust underlying the basin are favoured (1) by the hydrostatic pressure deficit of the basin and (2) by the disturbed crust consisting of fallback breccia in the upper part and a ruptured zone in the lower part, down to the mantle and, perhaps, reaching into the upper mantle. A relative density increase with regard to the undisturbed crust, of from 0.2 at the uppermost crust to 0.4 g/cm^3 at the Moho, is introduced for the crust-mantle mix. This two-body model requires an initial basin depth of only a few kilometers, in agreement with the estimation of Head et al. (1975) due to its thin mare basalt layer of 3.5 km.

All previous model types are combined in the three-body model suggested last (Fig. 3e): (1) a mare basalt thickness of 6 km, in agreement with the boundary condition of a thin mare basalt layer, (2) a mixed crust with a density increase of 0.2 g/cm^3, and (3) a moderately sized mantle plug of 12 km. Based on this model, an example of a complete model for Serenitatis and Crisium, together with measured and computed gravity anomalies, is presented in Fig. 4.

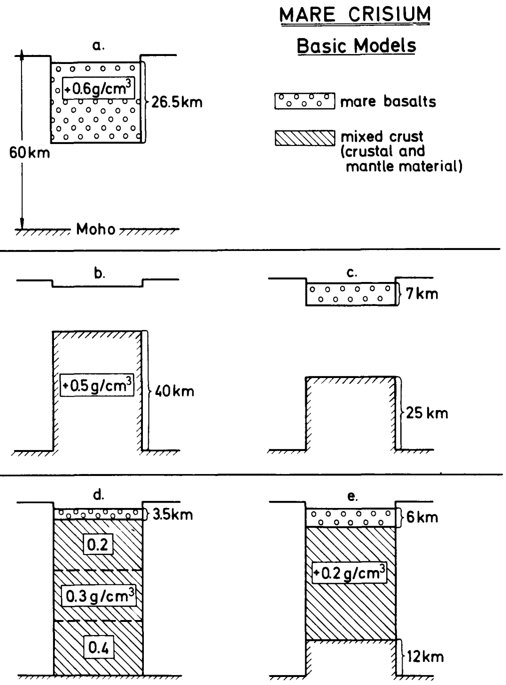

Fig. 3a–e. Basic gravity model solutions of Crisium (all calculated models include a mass model of Serenitatis), Apollo 15 CSM, Rev. 15. **a** Mare basalts (Conel and Holstrom 1968); **b** mantle plug (Wise and Yates 1970); **c** mare basalts and mantle plug (Bowin et al. 1975); **d** mare basalts and mixed crust (consisting of crustal and mantle material); **e** mare basalts, mixed crust, and mantle plug. (**a**, **b**: one-body models; **c**, **d**: two-body models; **e**: three-body model)

An Isostatic Model Solution

Non-isostatic mascon models cause considerable stress differences in the crust and mantle (Figs. 9 and 10). That is, the mass surpluses should have sunk into the mantle since their formation about 3×10^9 years ago, if the viscosity of the upper mantle is low. This may be the case for some high temperature models which have near-solidus temperatures at a depth of 200 km (Kuckes 1974; Sonett and Duba 1975). Isostatic modesl circumvent this problem provided that the depth of compensation lies far enough above the zone of near-solidus temperatures. Thus, the schematic solution pursued here aimed to find a minimum level of compansation.

Isostatic mascon models have already been proposed in earlier papers (Hulme 1972; Kunze 1974). They require that $\int_0^{z_0} g(z)\,\Delta\rho(z)\,dz$ where $\Delta\rho(z)$ = lateral density contrast, $g(z)$ = gravity, and z = depth, vanishes at the depth of isostatic compensation z_0. In order to account for the positive gravity anomaly of the mascons, the following restrictions on $\Delta\rho(z)$ are imposed: there must be compensating (1) surplus masses near to the surface producing larger gravity anomalies than observed, (2) there must be compensating mass deficits at depth, whose negative gravity anomalies at the altitude of observation are small compared to the positive anomaly due to the distance effect. The mass deficit due to the topographic depression of the mare surface leads to a further increase of the necessary mass surplus and depth of the mass deficit, respectively.

Kunze (1974) proposed a partial melt of the upper mantle below the basins due to pressure relief after basin excavation. Some melts rise up into the basins leaving a residuum of lower density which represents the compensating deficit mass. The depth

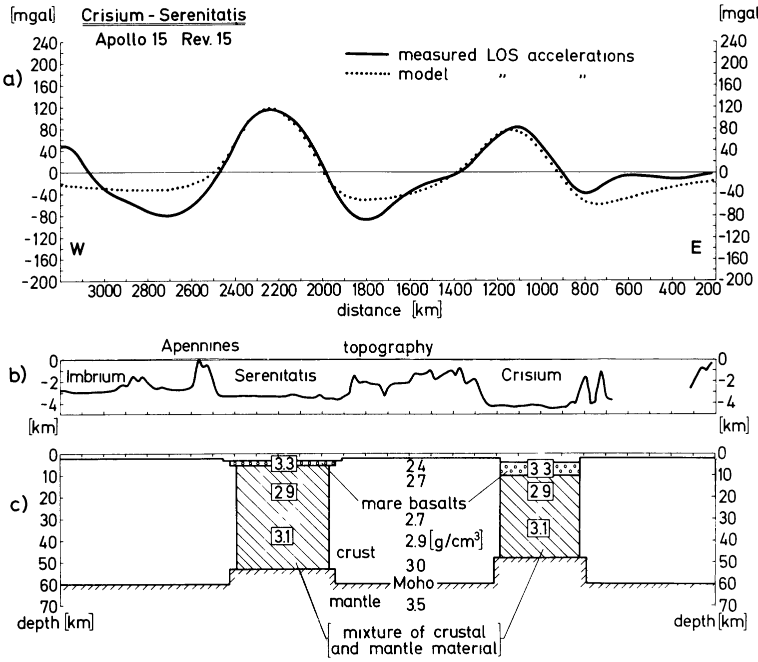

Fig. 4a–c. Model of mare basalts, mixed crust, and mantle plug for Serenitatis and Crisium, Apollo 15 CSM, Rev. 15; zero level of elevation and depth scales is related to a mean lunar radius of 1,738 km.
a Measured and model LOS accelerations;
b topography;
c density model

of compensation in this model lies at 450 km, which is not in agreement with the high temperature models mentioned above. Nevertheless, the possible existance of a compensating body lying higher is not in contradiction to the model history of Kunze.

Hulme (1972) proposed a model which was based mainly on gravitational sinking due to basin loading with heavy mare basalts. Thus, light crustal material is bent down into the higher density mantle causing a compensating body of negative density difference. The depth of compensation in this model lies at 150 km (with the assumption of a mean crustal thickness of 100 km), which is considerably above the zone of near solidus temperatures of the high temperature models.

In this paper, ignoring first the conception of a model history, a minimum depth solution for Crisium has been investigated. For this purpose, the upper limit of 7 km thickness for the mare basalts has been suspended. The mass surpluses of the mare basalts are compensated by an underlying body with negative density contrast to the surroundings of -0.5 g/cm^3

Every attempt failed to achieve isostatic compensation above the depth of the crust-mantle boundary. The final model led to a rather extreme solution with a mare basalt thickness of 60 km with an underlying zone of decreased density down to a depth of 116 km.

The following model history is proposed (compare Fig. 5): An initial basin depth of 100 to 150 km is assumed, consistent with the estimation of Dence (1977). About half the basin was filled with brecciated crustal and mantle material immediately after basin excavation, partly by fallback and partly by basin collapse. The remaining basin was subsequently flooded by mare basalts. Before basin flooding the density of the brecciated zone was 2.5 g/cm^3 or less (Talwani et al. 1973; Cooper et al. 1974). Intrusions of mantle material and later the pressure of the excess masses of the superimposed mare basalts caused a density increase in this zone, up to 3.0 g/cm^3, i.e., the density difference between these compensation masses and the undisturbed upper mantle is -0.5 g/cm^3

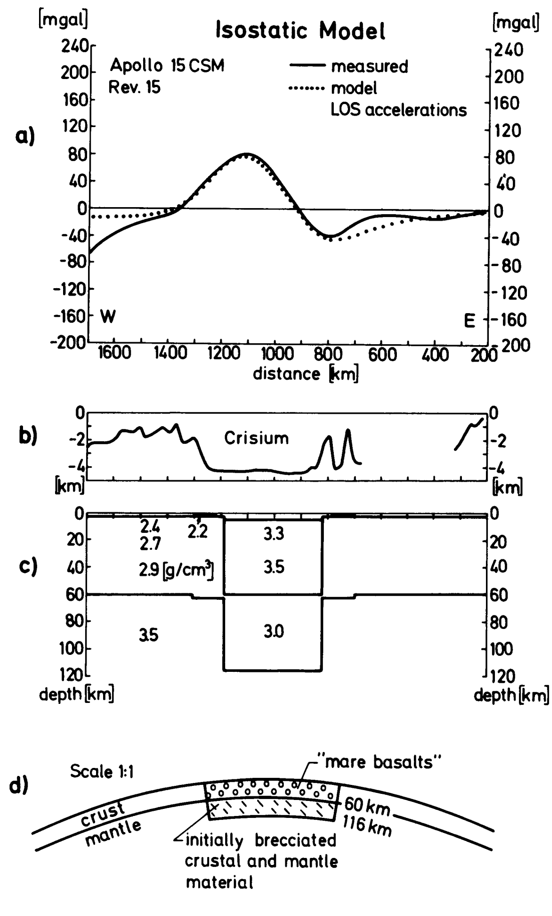

Fig. 5a–d. Isostatic model solution for Crisium, Apollo 15 CSM, Rev. 15. **a** Measured and model accelerations; **b** topography; **c** density model; **d** density model scaled 1 : 1

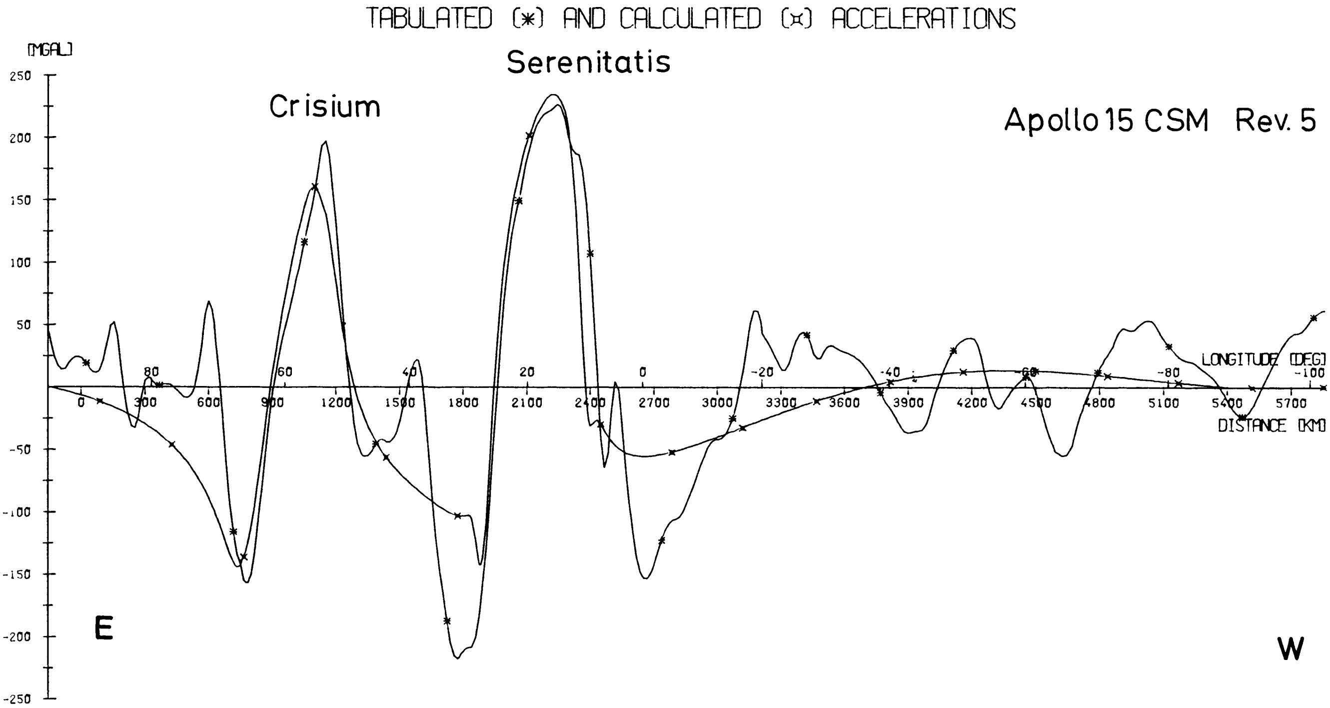

Fig. 6. Calculated gravity of the three-body model of Fig. 3e for Crisium and Serenitatis relating to the orbit of *Apollo 15 CSM, Rev. 5;* no additional fit to gravity of Rev. 5 (tabulated = measured, calculated = model LOS accelerations)

The isostatic model proposed here is very similar to the isostatic solution of Hulme (1972), however, the model histories are partly different.

Model Calculations for the Low Altitude Orbit and Model Discrimination

A strong restriction on the model solutions is given by the boundary condition of thin mare basalts, which rules out the pure basalt model (Fig. 3a) and the isostatic model (Fig. 5).

The model fits described above for revolution 15 have shown that many mass configurations satisfy the measured gravity data. This reflects the ambiguity of the gravity inverse problem. In order to achieve a further discrimination of different model solutions and to select a type for a final complete profile, the LOS gravity of all models presented above has also been computed for the low altitude orbit of Apollo 15 CSM, revolution 5. An example of these calculations is given in Fig. 6. The differences between computed and measured gravity maxima of Crisium and Serenitatis are listed in Table 2.

The model calculations show that the large gravity minima bordering the maria Imbrium, Serenitatis, and Crisium are only partly caused by negative boundary effects of the mascons (Figs. 4 and 6). This problem will be treated in the next section, in connection with a final model solution.

Table 2 shows that model fitting at two different altitudes does not constrain model discrimination significantly. There are still enough free parameters (density differences, height of mantle plug, horizontal extent of mass anomalies) which can be varied in order to fit the gravity anomalies in both orbital altitudes (Compare also differences of measured and calculated gravity of Fig. 6). Thus, the most stringent boundary condition is the upper limit for mare basalt thicknesses of 7 km. As mentioned above, the consideration of the topographic basin also greatly influences the model structure because it considerably increases the gravity anomalies which have to be fitted (Fig. 2).

Table 2. Apollo 15 CSM, Rev. 5. Differences between measured and model gravity maxima, mass distributions of Fig. 3, no additional fit to gravity of Rev. 5

Model type	Serenitatis (max. = 227 mgal)	Crisium (max. = 197 mgal)
Fig. 3		
(a) Mare basalts	38	15
(b) Mantle plug	37	26
(c) Mare basalts + mantle plug	7	50
(d) Mare basalts + mixed crust	−39	45
(e) Mare basalts + mantle plug + mixed crust	− 5	44
Isostatic model (only fit for Crisium, Fig. 5)	–	1

The isostatic model calculated for Crisium only can be excluded because of the extreme mare basalt thickness of 60 km, although it provides an excellent fit to the low altitude gravity data (Table 2).

Considering now the non-isostatic models, both one-body models can be excluded. In one case the mare basalt model (Fig. 3a) with a basalt thickness of 26.5 km is in contradiction to the boundary condition of a thin mare basalt layer. In the other case the mantle plug model (Fig. 3b) is in contradiction to the observed existence of high density basalts with a thickness of at least two kilometers. Another objection to this model is the requirement of an extremely high mantle plug of 40 km, i.e.,

$^2/_3$ of crustal thickness. Both two-body models (Figs. 3c, d) and the three-body model (Fig. 3e) agree with the boundary condition of thin mare basalt thicknesses.

The two-body model, combining a mixed crust and mare basalts (Fig. 3d), differs only slightly from the three-body model. The lower part of the mixed crust with a density difference of 0.4 g/cm^3 can also be interpreted as a mantle plug with minor crustal constituents. Thus, a discrimination between these two models is no longer necessary.

A discrimination between the two-body mare basalt/mantle plug model and the three-body model will now be suggested in relation to basin evolution processes. The mantle plug of 25 km in the two-body model seems to be rather large, but it cannot be excluded in view of rebound processes. The introduction of a zone of crust-mantle mix seems to be reasonable considering the following two processes during basin evolution. (1) in the case of an initial cavity deeper than crustal thickness (Dence 1977) a material mixing results in a crust-mantle mix below the basin, (2) during the mare basalt period, mantle material has intruded into the fractured region below the basins and finally flowed out into the basins; these mantle intrusions result in a density increase below the basins. The introduction of a zone of a crust-mantle mix leads, consequently, to a decrease of the mantle plug, comparing the two-body and the three-body models (Fig. 3c, e).

Summarizing the arguments above leads to the conclusion that the three-body model agrees best with the boundary conditions and the processes of basin building and mascon evolution. This model solution will be developed to a complex model in the next section.

A Complete Crustal Model from Southern Imbrium Over Serenitatis to Crisium

The main problems for a complete model fit of the measured gravity data extending from southern Imbrium over Serenitatis to Crisium are the large regional minima bordering the mascon anomalies (Figs. 4 and 6). They are caused partly by negative boundary effects from the mascons. Ferrari et al. (1978) proposed a crustal thickening between Imbrium and Serenitatis due to rebound processes after the impacts. This model is confirmed by a terrestrial experimental high-explosive crater (Snowball Crater, Roddy 1976, Fig. 15). The idea of crustal thickening has been adopted here. It has been modelled by several discs with a negative density contrast of -0.5 g/cm^3 The maximum thickening necessary is 20 km. In order to include the negative boundary effects of Imbrium on the western shores of Serenitatis, this mascon had also to be considered in the model configuration. The entire model was fitted to both the high and low altitude orbits (Figs. 7 and 8).

The final crustal model presented here gives a solution satisfying the gravity data of high and low altitude profiles for a rather large area with an extent of 3,000 km, i.e., long distance effects of the mascons of Imbrium, Serenitatis and Crisium and of the crustal thickenings are considered. The introduction of a mixed crust has the advantage of avoiding extremely thick mare basalts and large mantle plugs.

Conclusions

Considering the problem of isostasy of the complex model presented here, the central mascon area with its high positive lithostat-

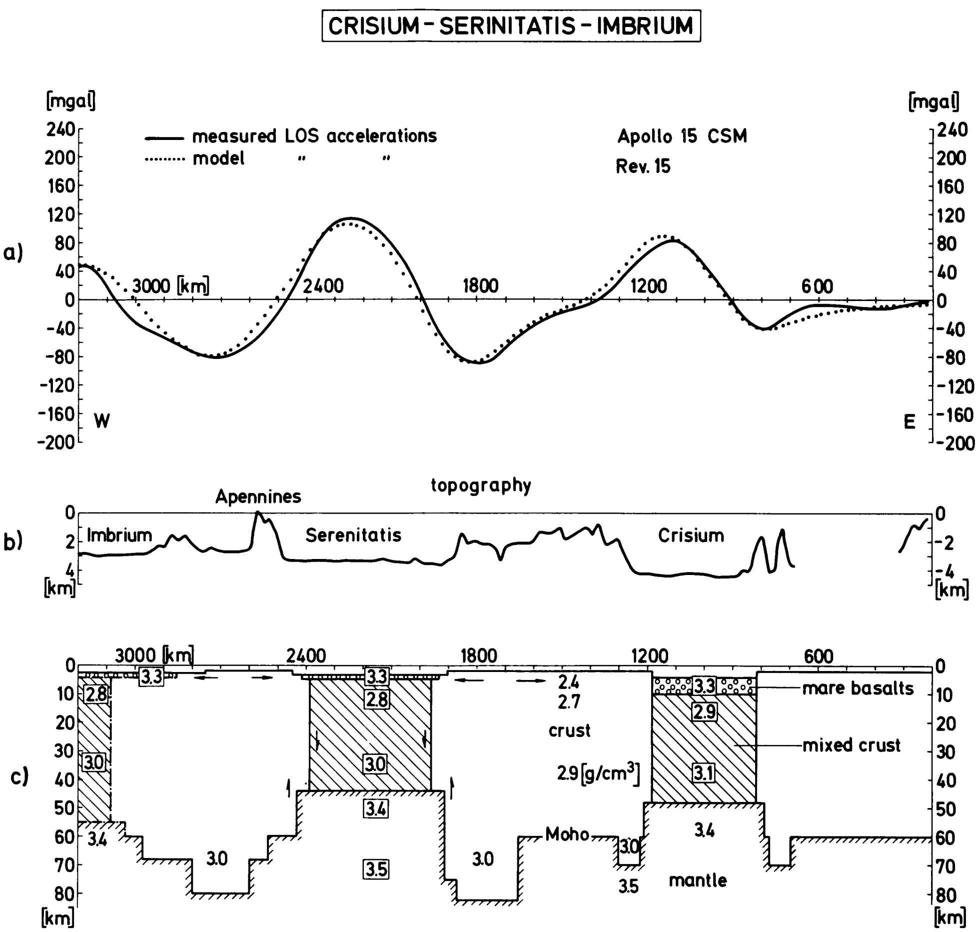

Fig. 7a–c. Complete crustal model from southern Imbrium over Serenitatis to Crisium, *Apollo 15 CSM, Rev. 15.* **a** Measured and model accelerations; **b** topography; **c** density model (*half arrows* indicate tendencies of crustal uplift and sinking, *full arrows* indicate areas of extensional surface stresses)

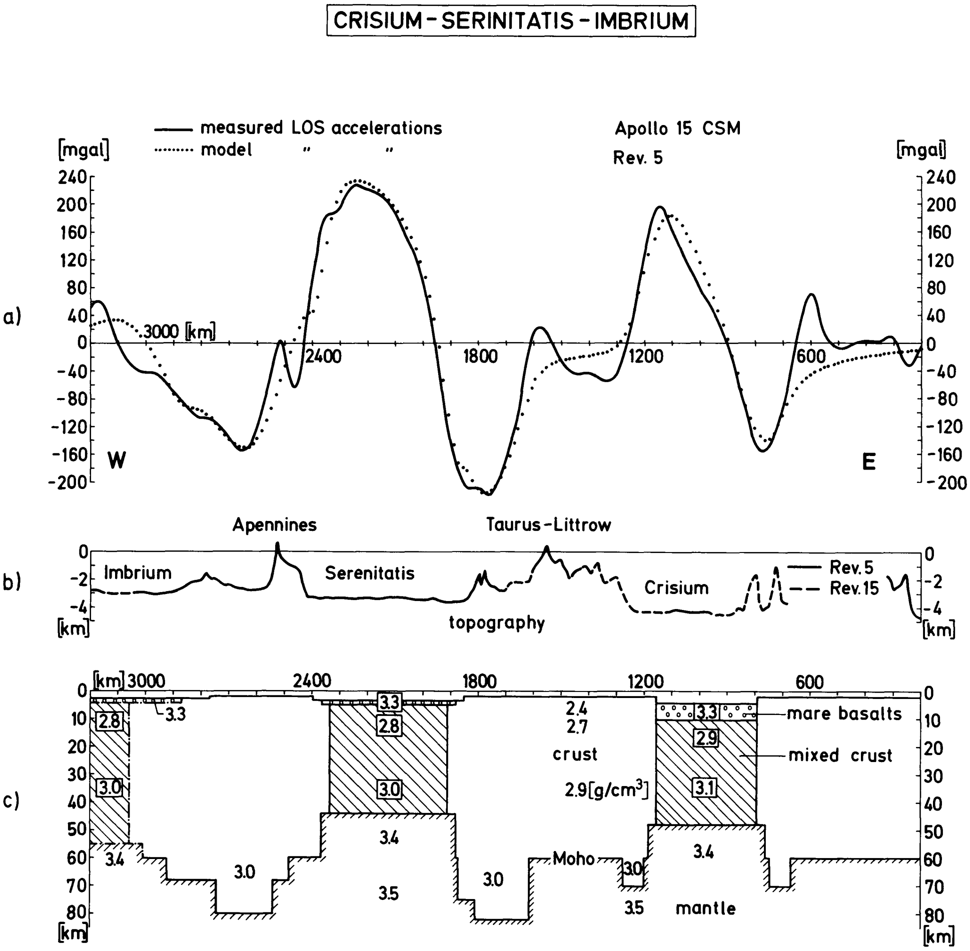

Fig. 8 a–c. Complete crustal model from southern Imbrium over Serenitatis to Crisium, *Apollo 15 CSM, Rev. 5.*
a Measured and model accelerations;
b topography;
c density model

ic stresses of 150–180 bar (Fig. 9) should have a tendency to crustal sinking (mass surpluses are associated in this paper with positive lithostatic stresses, mass deficits with negative stresses).

Compensation of the mass deficits of the 20 km crustal thickenings should result in a surrounding mountain range with an elevation of 4.2 km. From the elevation profiles of Figs. 7 and 8, there is no indication, in the areas of crustal thickening, of such large mountain ranges; i.e., the mass deficits are more or less uncompensated. Assuming a density difference of -0.5 g/cm^3 leads to negative lithostatic stresses of -161 bars with an uplift tendency. This is the same order of magnitude as the positive stresses of the central mascon areas. Thus the contact zones of the areas of crustal sinking and uplift should be favoured for progressive tectonic failure zones.

These conclusions are in accordance with two morphologic structures: (1) the basin edges are favoured for the origin of the youngest lava flows (Boyce 1976); (2) the tendency to crustal sinking in the mascon area combined with the tendency to crustal uplift in the bordering zones results in an extensional stress field in the bordering zones, which may be the cause for the surrounding rilles of many maria (Fig. 7). Extensional stresses for the bordering zones of Serenitatis have been calculated by Solomon and Head (1979) based on a one-body mare basalt model. The crustal thickenings proposed in the model of this paper lead to a strengthening of the surrounding extensional stress field.

In the following the question of stability of non-isostatic mascon models is discussed.

Age determinations of mare basalts showed that the main phases of basin filling are terminated at about 3×10^9 years B.P., although many younger flows exist, up to 2.5×10^9 years B.P. (Boyce and Johnson 1978; Boyce 1976). This means that the lunar crust/mantle system must have been able to sustain lithostatic stresses of 160 to 180 bars (Fig. 9) for 3×10^9 years.

The lithostatic stresses acting on the mantle can be used (1) to estimate the upper mantle viscosity η and (2) to calculate the maximum shear stresses applied to the upper mantle.

(1) Considering the lunar mantle as a half space with the rheologic properties of a Maxwell body, the elastic and viscous parts can be decoupled for long loading times (Cathles 1975, pp. 59–60). Assuming a cylindrical load, the vertical elastic displacement u and the vertical viscous displacement velocity v for the center of the load are given by Nadai (1963), pp. 241–246):

$$u=\frac{(1-\sigma)P_z a}{k}$$

$$v=\frac{\Delta z}{\Delta t}=\frac{P_z a}{2}\qquad \eta=\frac{P_z a \Delta t}{2\Delta z}$$

where

P_z = load (lithostatic stress, Fig. 9)
a = radius of the load
σ = Poisson ratio
k = modulus of shear
Δz = vertical displacement of the load
Δt = loading time

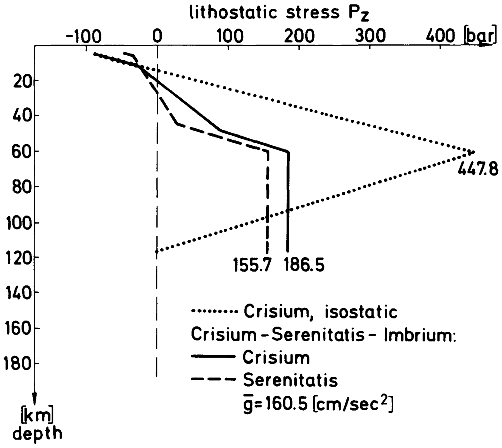

Fig. 9. Lithostatic stresses P_z of Serenitatis and Crisium (relating to mass distributions of Figs. 5 and 7). $\left(P_z=\bar{g}\sum_{i=1}^{n}\Delta\rho_i\Delta z_i;\ \bar{g}=\text{mean acceleration},\ n=\text{number of layers with density } \Delta\rho_i \text{ and thickness } \Delta z_i\right)$

A Poisson ratio of 0.25 is adopted from Nakamura et al. (1976). A shear modulus k of 7.7×10^{11} dyne/cm^2 is found using $k=\rho V_s^2$, with an upper mantle density ρ of 3.5 g/cm^3 used in this paper and an upper mantle shear wave velocity V_s of 4.7 km/s (Nakamura et al. 1976).

The vertical displacement Δz of the load results from elevation statistics of Runcorn (1974), who found a systematically lower level of 1 to 1.5 km of the circular maria relative to the irregular maria which are older and do not have excess masses.

All parameters used in displacement and viscosity calculations are summarized in Table 3.

The elastic displacement u is about 35 m for Crisium and Serenitatis. This value may be neglected in relation to 1 km of total sinking. An effective upper mantle viscosity of 10^{27} poise assumed constant for the whole time period of 3×10^9 years, is obtained. This value is in agreement with investigations of Arkani-Hamed (1973) for postmare viscosity and Meissner (1975).

In reality there should be a gradual increase of viscosity with time due to cooling; however the sparse data included in the estimations in this investigation do not justify evaluation of more detailed viscosity models.

(2) Maximum shear stresses (τ_{max}) applied to the upper mantle half space can be calculated from lithostatic stresses of Crisium and Serenitatis with the assumption of cylindrical loading (Fig. 9; Nadai 1963, p. 245):

$$\tau_{max}=(^1/_4)P_z(-1+2\sigma-2(1+\sigma)z(a^2+z^2)^{-1/2}+3z^3(a^2+z^2)^{-3/2}$$

z = depth

The resulting maximum shear stresses in the upper mantle are shown in Fig. 10.

These results have an important bearing on the lunar thermal history. The high average effective upper mantle viscosity of 10^{27} poise and the shear stresses of 65 bar at a depth of 200 km are not compatible with some temperature models (Kuckes 1974; Sonnett and Duba 1975) which are not more than about 200° K below the solidus at this depth. Considering a mantle solidus of about 1,600° K (T_m) at a depth of 200 km (Hodges and Kushiro 1974) a mantle temperature of 1,300° K (T) yields a relation

Table 3

Load P_z	Crisium	186.5 bar
	Serenitatis	155.7 bar
Radius a	Crisium	182 km
	Serenitatis	243 km
Poisson ratio		0.25
Shear modulus K		7.7×10^{11} dyne/cm^2
Loading time Δt		3×10^9 years
Vertical displacement Δz of the load		1 km

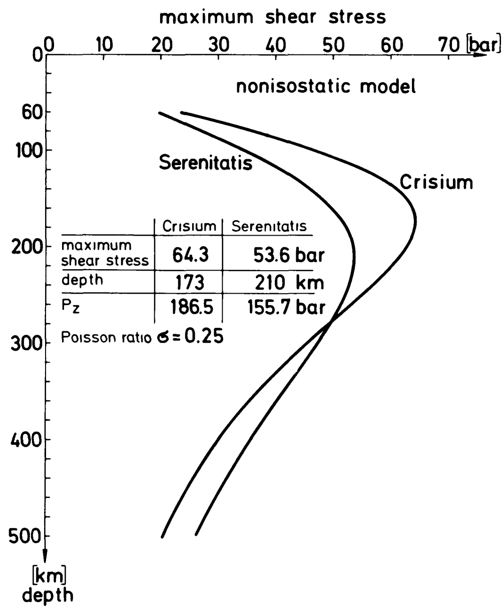

Fig. 10. Maximum shear stresses below Serenitatis and Crisium (relating to mass distributions of Fig. 7)

$T/T_m=0.8$. A conversion of T/T_m into viscosity, according to the method of Meissner and Lange (1977), gives a value of less than 10^{20} poise which is unreasonably low.

Turcotte (1979) developed a stress relaxation temperature T_e depending on an olivine deformation law:

$$T_e=\frac{6.16\times10^4}{\ln(2.62\times10^9\,\sigma_0^2\,t_r)}$$

(σ_0 = initial stress in bars, t_r = relaxation time in s, T_e in °K).

Assuming for the lunar case $\sigma_0=100$ bar and $t_r=10^9$ years gives in $T_e=900°$ K. This result shows that high temperature models are not compatible with significant mascon stresses. Recent calculations of upper mantle temperatures by Keihm and Langseth (1977), which vary from 300° K to 600° K below the solidus at a depth of 200 km, are more appropriate to a high upper mantle viscosity and the existence of significant shear stresses. Considering the estimation of the stress relaxation temperature above, the cooler values should be preferred.

The discussion above did not consider the effect of the absence of volatiles, especially water, in lunar materials. Laboratory investigations by Mitzutanni et al. (1977) and theoretical calculations by Kirby (1977) and Meissner (in press 1980), in the case of the Earth, show an increase of strength with decreasing water content of the materials. Since it seems impossible to extrapolate from terrestrial conditions to the moon, a repetition of these experimental and theoretical investigations under lunar conditions, especially under totally dry conditions, is necessary.

Acknowledgements. This study was sponsored by the Deutsche Forschungsgemeinschaft (German Research Society). I thank Dr. W.L. Sjogren, Jet Propulsion Laboratory in Pasadena, California, for leaving the program ORBISIM which made the model calculations possible. The gravity data from the Apollo missions were made available by World Data Center A in Greenbelt, Maryland. I want to thank Professor Dr. R. Meissner, Dr. A. Binder, and Dr. J. Voss, Kiel, for reading the manuscript and for helpful discussions. I am further indebted to J. Ropers, Hamburg, for computational support.

References

Andre, C.G., Wolfe, R.W., Adler, K., Clark, P.E.. Mare basalt depth from orbital X-ray data. Lunar Planet. Sci. **10**, 38–40, 1979

Arkani-Hamed, J.: Viscosity of the Moon I. The Moon **6**, 100–111, 1973

Boyce, I.M.: Ages of flow units in the lunar nearside maria based on Lunar Orbiter IV photographs. Proc. Lunar Sci. Conf. 7th, 2717–2728, 1976

Boyce, I.M., Johnson, D.A.: Ages of flow units in the eastern maria and Mare Humorum based on crater density. Lunar Planet. Sci. **9**, 117–119, 1978

Bowin, C., Simon, B., Wollenhaupt, W.R.: Mascons: A two-body solution. J. Geophys. Res. **80**, 4947–4955, 1975

Cathles, L.M., III: The viscosity of the earth's mantle. Princeton, New Jersey: Princeton University Press 1975

Conel, J.E., and Holstrom, G.B.: Lunar mascons: A near-surface interpretation. Science **162**, 1403–1405, 1968

Cooper, M.R., Kovach, R.L., Watkins, J.S.· Lunar near-surface structure. Rev. Geophys. and Space Phys. **12**, 291–308, 1974

De Hon, R.A., Waskom, J.D.: Geologic structure of the eastern mare basins. Proc. Lunar Sci. Conf. 7th, 2729–2746, 1976

Dence, M.R.: Meteoritic bombardment of the moon. Philos. Trans. R. Soc. London A. **285**, 259–265, 1977

Ferrari, A.J., Nelson, D.L., Sjogren, W.L., Phillips, R.J.: The isostatic state of the lunar Apennines and regional surroundings. J. Geophys. Res. **83**, 2863–2871, 1978

Gottlieb, P.: Estimation of local gravity features. Radio Sci. **5**, 303–312, 1970

Head, J.W., Settle, M., Stein, R.S.: Volume of material ejected from major lunar basins and implications for the depth of excavation of lunar samples. Proc. Lunar Sci. Conf. 6th, 2805–2829, 1975

Hodges, F.N., Kushiro, I.. Apollo 17 petrology and experimental determination of differentiation sequences in model moon composition. Proc. Lunar Sci. Conf. 5th, 505–520, 1974

Hörz, F.: How thick are lunar mare basalts? Proc. Lunar Sci. Conf. 9th, 3311–3331, 1978

Hulme, G.: Mascons and isostasy. Nature **238**, 448–450, 1972

Keihm, S.J., Langseth, M.G.: Lunar thermal regime to 300 km. Proc. Lunar Sci. Conf. 8th, 499–514, 1977

Kirby, S.H.: State of stress in the lithosphere: inferences from the flow laws of olivine. Pure Appl. Geophys. **115**, 245–258, 1977

Kuckes, A.F.: Lunar magnetometry and mantle convection. Nature **252**, 670–672, 1974

Kunze, A.W.G.: Lunar mascons: another model and its implications. The Moon **11**, 9–17, 1974

Meissner, R.: Lunar viscosity as obtained from the selenotherms. The Moon **12**, 179–191, 1975

Meissner, R.: Limits on stresses in continental crusts. J. Geophys. Res. in press, 1980

Meissner, R., Lange, M.: An approach for calculating temperatures and viscosities in terrestrial planets. Proc. Lunar Sci. Conf. 8th, 551–562, 1977

Michael, W.H., Blackshear, W.T : Recent results on the mass, gravitational field and moments of inertia of the moon. The Moon **3**, 388–402, 1972

Mizutanni, H., Spetzler, H., Getting, I., Martin, R.J., III, Soga, N.: The effect of outgassing upon the closure of cracks and the strength of lunar analogues. Proc. Lunar Sci. Conf. 8th, 1238–1248, 1977

Muller, P.M., Sjogren, W.L.: Mascons: Lunar mass concentrations. Science **161**, 680–684, 1968

Nadai, A.: Theory of flow and fracture of solids, vol. 2. New York, Toronto, London: McGraw-Hill 1963

Nakamura, Y., Latham, G.V., Dorman, H.J., Duennebier, F.K. Seismic structure of the moon: a summary of current status. Proc. Lunar Sci. Conf. 7th, 3113–3121, 1976

Phillips, R.J., Sjogren, W.L., Abbott, E.A.· Simulation gravity modelling to spacecraft-tracking data: analysis and application. J. Geophys. Res. **83**, 5455–5464, 1978

Roddy, D.J.: High-explosive cratering analogs for bowl-shaped, central uplift and multiring impact craters, Proc. Lunar Sci. Conf. 7th, 3027–3056, 1976

Runcorn, S.K.: On the origin of mascons and moonquakes. Proc. Lunar Sci. Conf. 5th, 3115–3126, 1974

Schimerman, L.A. (ed.): NASA lunar cartographic dossier, vol. 1. St. Louis: Defense Mapping Agency, Aerospace Center 1973

Sjogren, W.L., Anderson, J.D., Phillips, R.J., Trask, D.W.: Gravity fields. IEE transactions on Geoscience electronics, **GE-14**, 1972–183, 1976

Sjogren, W.L., Smith, J.C.: Quantitative mass distribution models for Mare Orientale. Proc. Lunar Sci. Conf. 7th, 2639–2648, 1976

Solomon, S.C.: Density within the moon and implications for lunar composition. The Moon **9**, 147–166, 1974

Solomon, S.C., Head, J.W.: Vertical movement in mare basins: relation to mare emplacement, basin tectonics, and lunar thermal history. J. Geophys. Res. **84**, 1664–1682, 1979

Sonnett, C.P., Duba, A.: Lunar temperature and global heat flux from laboratory electrical conductivity and lunar magnetometer data. Nature **258**, 118–121, 1975

Talwani, M., Thompson, G., Dent, B., Kahle, H.-G., Buck, S.: Traverse gravimeter experiment. In: Apollo 17, Preliminary Science Report. NASA SP-330, 13-1-13-13, 1973

Toksöz, M.N., Press, F., Dainty, A.M., Anderson, K.R.: Lunar velocity structure and compositional and thermal inferences. The Moon **9**, 31–42, 1974

Turcotte, D.L.: Flexure. Adv. Geophys. **21**, 51–86, 1979

Wise, D.U., Yates, M.T : Mascons as structural relief on a lunar "Moho" J. Geophys. Res. **75**, 261–268, 1970

Received September 18, 1979; Revised Version March 13, 1980
Accepted July 2, 1980